

Excitonic instability of three-dimensional gapless semiconductors: Large- N theory

Lukas Janssen and Igor F. Herbut

Department of Physics, Simon Fraser University, Burnaby, British Columbia, Canada V5A 1S6

Three-dimensional gapless semiconductors with quadratic band touching, such as HgTe, α -Sn, or $\text{Pr}_2\text{Ir}_2\text{O}_7$ are believed to display a non-Fermi-liquid ground state due to long-range electron-electron interaction. We argue that this state is inherently unstable towards spontaneous formation of a (topological) excitonic insulator. The instability can be parameterized by a critical fermion number N_c . For $N < N_c$ the rotational symmetry is spontaneously broken, the system develops a gap in the spectrum, and features a finite nematic order parameter. To leading order in the $1/N$ expansion and in the static approximation, the analogy with the problem of dynamical mass generation in (2+1)-dimensional quantum electrodynamics yields $N_c = 16/[3\pi(\pi - 2)]$. Taking the important dynamical screening effects into account, we find that $N_c \geq 2.6(2)$ and therefore safely above the physical value of $N = 1$. Some experimental consequences of the nematic ground state are discussed.

I. INTRODUCTION

Three-dimensional (3D) Fermi systems in which valence and conduction bands touch quadratically at the Fermi level form the very boundary between two classes of materials: Right at the Fermi level their density of states vanishes and the systems can hence be understood as limiting cases of semiconductors in which the band gap goes to zero. Away from the Fermi level, on the other hand, the density of states increases rapidly, and the systems may alternatively be regarded as degenerate semimetals with the band overlap region shrunk to a single point. Prominent examples for such three-dimensional *gapless semiconductors* are given by α -Sn and HgTe, which feature band inversion due to spin-orbit coupling. The quadratic band touching (QBT) point, located at the center Γ of the Brillouin zone, is protected by crystal symmetry, and in the undoped systems the Fermi level is right at the touching point [1]. When the rotational symmetry is broken, the band degeneracy at the Γ point can be lifted and the spectrum develops a full, anisotropic, and topologically nontrivial gap [2]. HgTe, for instance, shows the quantum spin Hall effect in quantum well structures [3] and becomes a 3D strong topological insulator under uniaxial strain [4]. The pyrochlore iridates $R_2\text{Ir}_2\text{O}_7$ (where R is a rare-earth element) that display a metallic paramagnetic state presumably also host a 3D QBT point at the Fermi level [5, 6]. This scenario has been employed to explain the anomalous low-temperature behavior measured in $\text{Pr}_2\text{Ir}_2\text{O}_7$ [7].

The dichotomous classification of gapless semiconductors is reflected in their concomitant peculiar *marginal* screening, which allows fundamentally new types of many-body ground states. Theoretical control over the situation can be exerted by employing a $1/N$ expansion, where N is the number of QBT points at the Fermi level. In the limit of large N , Abrikosov and Beneslavskii found a scale-invariant semimetallic ground state with anomalous power laws—a 3D non-Fermi-liquid phase [8]. Recently, their analysis has been rediscovered and extended in the context of the pyrochlore iridates [7].

In this work, we revisit the problem of the ground

state of 3D Fermi systems with QBT by deriving and exploiting the nonperturbative solution of the Dyson-Schwinger equations. Although also controlled by the small parameter $1/N$, this enables one to address questions such as spontaneous symmetry breaking and dynamical mass generation. We demonstrate that the Abrikosov-Beneslavskii large- N regime exhibits a lower bound N_c below which the non-Fermi-liquid state becomes unstable and the system features a symmetry-breaking phase transition. The value for N_c is found to be *above* the physical $N = 1$, rendering the 3D systems with QBT insulating and nematic at low temperatures. While such a possibility has been suggested earlier by considering the theory in higher spatial dimensions $d > 3$ [9], so far there has not been a definite demonstration of the instability within a fully controlled approximation. Conceptually, our scenario is analogous to the well-known situation in (2+1)-dimensional quantum electrodynamics (QED₃), which displays chiral symmetry breaking if the number of fermions is less than a certain critical fermion number [10–14]. The principal difference is, however, the lack of relativistic invariance at low energies, which makes the effects of dynamical screening both crucial and nontrivial to include. We show, nevertheless, that the critical number of four-component fermions N_c is, to the leading order of the $1/N$ expansion, bounded from below by 2.6(2), and thus is significantly larger than the relevant physical value of $N = 1$.

II. SEMICLASSICAL PICTURE

The N -dependent excitonic transition can be understood heuristically within a simple semiclassical picture. At the Fermi level, the point of QBT separates the filled valence electron band from the unoccupied conduction band. Virtual or thermal fluctuations can induce electron-hole pairs, which interact via an attractive screened Coulomb potential $V(r)$. In the simplest approach, the latter is determined by the density of

states $\rho(\varepsilon_{\vec{p}})$ near the Fermi level [15],

$$V(r) = \int \frac{d^3\vec{p}}{(2\pi)^3} \frac{e^{i\vec{r}\cdot\vec{p}}}{\frac{p^2\kappa}{4\pi e^2} + \rho(\varepsilon_{\vec{p}})}, \quad (1)$$

where e is the elementary charge and κ is the “background” dielectric constant arising from transitions between bands away from the Fermi level [16]. When the band dispersion is quadratic, $\varepsilon_{\vec{p}} \propto \pm p^2$, the density of states vanishes linearly as a function of momentum, $\rho(\varepsilon_{\vec{p}}) \propto N|\vec{p}|$, with N the number of QBT points at the Fermi level. At large distances, the form of the potential thus becomes $\propto 1/p$ in Fourier space or, equivalently, $V(r) \propto 1/r^2$ in real space. The Coulomb interaction is *marginally* screened, in clear contrast to both metallic and dielectric screening. Whether or not an electron-hole pair can form an excitonic quasiparticle is determined by the spectrum of the corresponding s -wave Schrödinger equation for the radial “exciton wave function” $\Psi_{\text{exc}}(r)$,

$$\left[-\frac{1}{r^2} \frac{d}{dr} \left(r^2 \frac{d}{dr} \right) - \frac{\alpha}{N} \frac{1}{r^2} \right] \Psi_{\text{exc}}(r) = 2mE \Psi_{\text{exc}}(r), \quad (2)$$

where m is the effective band mass, α is a dimensionless constant, and we have set $\hbar = 1$. An exciton bound state would be given by the solution of Eq. (2) with energy eigenvalue $E < 0$. The quantum mechanical Hamiltonian with $1/r^2$ potential is formally invariant under the scale transformation $r \mapsto \beta r$, $\beta > 0$. A discrete bound-state spectrum would inevitably break the scale invariance, and one therefore might expect the spectrum to possess scattering states only. This naive expectation, however, is correct only for weak interaction, when the dimensionless parameter $\alpha/N < 1/4$ [17]. In this case, no exciton formation is possible, and the 3D QBT system becomes scale invariant at large distances. This is the Abrikosov-Beneslavskii non-Fermi-liquid state [7, 8]. For $\alpha/N > 1/4$, on the other hand, the Hamiltonian needs to be regularized at short distances and *does* admit bound states, with energy eigenvalues $E < 0$ that depend on the regularization [18]. This peculiarity of the quantum mechanics of the attractive $1/r^2$ potential can be interpreted as possibly the simplest realization of a quantum anomaly [19]. In our system, screening is suppressed at short distances, which naturally regularizes the potential and prevents the electron-hole pair from “collapsing” [17]. For small values of N , exciton formation is thus possible and in fact favored energetically. The critical number of fermions that separates the scale-invariant non-Fermi-liquid phase at large N from the excitonic insulating phase at small N would in this approximation be given by $N_c = 4\alpha$.

In what follows we use the field-theoretical machinery to demonstrate that the above picture is qualitatively entirely correct. In particular, we will find that the system can be described by a differential equation formally identical to Eq. (2), with a value for α that leads to $N_c > 1$.

III. FIELD THEORY FOR 3D QBT SYSTEM

The minimal low-energy Hamiltonian relevant for semiconductors with diamond or zincblende crystal structure is given by the Luttinger Hamiltonian [20, 21]

$$\mathcal{H}_0(\vec{p}) = \frac{1}{2m} \left[(\alpha_1 + \frac{5}{2}\alpha_2) p^2 \mathbb{1}_4 - 2\alpha_2 (\vec{p} \cdot \vec{J})^2 \right], \quad (3)$$

with \vec{J} as the (4×4) $j = 3/2$ representation of the angular momentum algebra, α_i the phenomenological Luttinger parameters, and where we assumed spherical symmetry. The spectrum then is $\varepsilon_{\vec{p}} = (\alpha_1 \pm 2\alpha_2) p^2 / (2m)$, and \mathcal{H}_0 describes a QBT point if $|\alpha_1| < 2|\alpha_2|$. For large N , both spherical as well as particle-hole symmetry are in fact expected to be *emergent* at low energies [7], and for simplicity we therefore also set $\alpha_1 = 0$ in the following. While the assumption of spherical symmetry appears to be a valid description of HgTe and α -Sn [1], we should note that strong correlations in the pyrochlore iridates may induce significant anisotropies [22]. For a quantitative description of the latter systems it may therefore be necessary to go beyond our simple rotationally and particle-hole symmetric model. This is left for future work.

The Hamiltonian can then be written as [23]

$$\mathcal{H}_0(\vec{p}) = \sum_{a=1}^5 d_a(\vec{p}) \gamma_a, \quad (4)$$

where $d_a(\vec{p}) = p^2 \tilde{d}_a(\vartheta, \varphi)$ are the five real spherical harmonics for the angular momentum of two, viz., $\tilde{d}_1 + i\tilde{d}_2 = (\sqrt{3}/2) \sin^2(\vartheta) e^{2i\varphi}$, $\tilde{d}_3 + i\tilde{d}_4 = (\sqrt{3}/2) \sin(2\vartheta) e^{i\varphi}$, and $\tilde{d}_5 = (3 \cos^2 \vartheta - 1)/2$, with ϑ and φ as the spherical angles in momentum space. The Hermitian 4×4 Dirac matrices $\gamma_1, \dots, \gamma_5$ satisfy the Clifford algebra $\{\gamma_a, \gamma_b\} = 2\delta_{ab}$. For convenience, in Eq. (4) we have also set the remaining effective band mass to $m/\alpha_2 = 1$.

We are interested in the effects of the long-range Coulomb interaction, which is mediated by a scalar field a , and described by the Euclidian bare action

$$S = \int d\tau d^3\vec{x} \left[\psi_i^\dagger (\partial_\tau + ia + \mathcal{H}_0) \psi_i + \frac{1}{2e^2} (\nabla a)^2 \right]. \quad (5)$$

ψ_i and ψ_i^\dagger are four-component fermion fields, and $i = 1, \dots, N$. Upon integrating out a in the functional integral, the bare $1/r$ density-density interaction is recovered.

\mathcal{H}_0 contains the complete set of *five* anticommuting 4×4 Dirac matrices; there is no further matrix left that would anticommute with all matrices present in the Hamiltonian. An isotropic mass gap, that is usually energetically favored in systems with Dirac fermions [24] and in two-dimensional QBT models [25], is thus impossible in the (isotropic) 3D systems with QBT. This leaves as the energetically next-best option the full, but *anisotropic* mass gap $\Delta \propto \langle \psi^\dagger \gamma_5 \psi \rangle$ [9], which can be

understood as nematic order parameter [23]. As a genuine many-body phenomenon, dynamical mass generation is inaccessible to perturbation theory. Similarly to QED₃ [10–12] and graphene [26–28], a possible excitonic instability can, however, be revealed by a nonperturbative solution of the gap equation for the fermion Green's function $G(\omega, \vec{p})$,

$$G^{-1}(\omega, \vec{p}) = i\omega + \mathcal{H}_0(\vec{p}) + \int \frac{d\nu d^3\vec{q}}{(2\pi)^4} [\Gamma(\omega, \vec{p}; \nu, \vec{q}) \times G(\nu, \vec{q}) V(\nu - \omega, \vec{q} - \vec{p})], \quad (6)$$

involving the full vertex function $\Gamma(\omega, \vec{p}; \nu, \vec{q})$ and Coulomb Green's function $V(\omega, \vec{p})$. The latter in turn is screened by the fermion polarization,

$$V^{-1}(\omega, \vec{p}) = \frac{p^2}{e^2} - N \int \frac{d\nu d^3\vec{q}}{(2\pi)^4} \text{tr} [\Gamma(\omega + \nu, \vec{p} + \vec{q}; \nu, \vec{q}) \times G(\omega + \nu, \vec{p} + \vec{q}) G(\nu, \vec{q})]. \quad (7)$$

Similarly, the vertex function fulfills an equation that involves the fermion four-point function, and in general this leads to an infinite tower of coupled functional integral equations—the Dyson-Schwinger equations. Within the $1/N$ expansion, the set of equations can be solved successively. The wave-function renormalization has the expansion $Z(\omega, \vec{p}) = 1 + \mathcal{O}(1/N)$ [10], and to the leading order the fermion Green's function becomes

$$G(\omega, \vec{p}) = [i\omega + d_a(\vec{p})\gamma_a + \Delta(\omega, \vec{p})\gamma_5]^{-1}, \quad (8)$$

where we have assumed the effective band mass to be already at its renormalized value [29]. In Eq. (8) and hereafter we adopt the summation convention over repeated indices. The vertex renormalization is also suppressed by $1/N$, $\Gamma(\omega, \vec{p}; \nu, \vec{q}) = 1 + \mathcal{O}(1/N)$ [10]. In QED₃, higher-order calculations give corrections to N_c of no more than 25% [11, 12], and it is therefore reasonable to expect the relevant physics in the present case also to be captured well already by the lowest-order calculation.

We first discuss the solution in the intermediate range of momenta $\Delta(\omega, \vec{p}) \ll p^2 \ll e^4$, in which the gap equation can be linearized. This assumption will be justified *a posteriori* in the limit $N \rightarrow N_c$. The screened Coulomb potential in this regime is, to leading order in $1/N$,

$$V^{-1}(\omega, \vec{p}) = 4N \int_{\nu, \vec{q}} \frac{\nu(\nu + \omega) - d_a(\vec{q})d_a(\vec{p} + \vec{q})}{(\nu^2 + q^4)[(\nu + \omega)^2 + (\vec{p} + \vec{q})^4]}, \quad (9)$$

where we abbreviated $\int_{\nu, \vec{q}} \equiv \int \frac{d\nu d^3\vec{q}}{(2\pi)^4}$. Carrying out the integration gives

$$V(\omega, \vec{p}) = \frac{1}{N|\vec{p}|} \mathcal{F}\left(\sqrt{\frac{|\omega|}{p^2}}\right), \quad (10)$$

with the dimensionless scaling function \mathcal{F} ,

$$\mathcal{F}(x) \simeq \begin{cases} \frac{16\pi}{3(\pi-2)} & \text{for } x \ll 1, \\ 4\pi x & \text{for } x \gg 1, \end{cases} \quad (11)$$

and interpolating monotonically between these two limits for intermediate x .

IV. STATIC APPROXIMATION

In the static approximation screened potential $V(\omega, \vec{p})$ and gap function $\Delta(\omega, \vec{p})$ are approximated by their values at $\omega = 0$. Note that in real space then $V(r) \propto 1/r^2$, as anticipated above. If we furthermore assume $\Delta(\vec{p}) \equiv \Delta(|\vec{p}|)$, the integral over frequency and spherical angles in the gap equation (6) gives

$$N\Delta(p) = \frac{4}{3\pi(\pi-2)} \int_{\lambda}^{\Lambda} dq \frac{\Delta(q)}{\max(p, q)}, \quad (12)$$

where $\Lambda \approx e^2$ and $\lambda \approx \sqrt{\Delta(0)}$ are the UV and IR cutoffs, respectively. This integral equation for $\Delta(p)$ is equivalent to the differential equation [10]

$$\left[\frac{d}{dp} \left(p^2 \frac{d}{dp} \right) + \frac{4}{3\pi(\pi-2)N} \right] \Delta(p) = 0, \quad (13)$$

supplemented with the boundary conditions

$$\lim_{p \rightarrow \infty} \left(p \frac{d\Delta(p)}{dp} + \Delta(p) \right) = 0 \quad \text{and} \quad \lim_{p \rightarrow 0} \Delta(p) < \infty. \quad (14)$$

We note that Eq. (13) is formally identical to the exciton bound-state equation (2) for $E = 0$. The very same differential equation (13) together with the boundary conditions (14) appear also in the leading-order solution of the Dyson-Schwinger equations in QED₃ [10], quenched QED₄ [30], and graphene [26, 27]. We hence simply adopt the results for the present model. For $N > N_c = 16/[3\pi(\pi-2)]$ the unique solution to Eqs. (13) and (14) is the trivial one, $\Delta(p) \equiv 0$. For $N < N_c$, in contrast, the equations admit the oscillatory solution

$$\Delta(p) \propto \frac{1}{\sqrt{p}} \sin \left[\frac{1}{2} \sqrt{\frac{N_c}{N}} - 1 \ln \left(\frac{p}{\sqrt{\Delta(0)}} \right) \right], \quad (15)$$

valid for momenta $\Delta(0) \ll p^2 \ll e^4$, and with

$$\Delta(0) \propto \exp \left(\frac{-4\pi}{\sqrt{N_c/N - 1}} + \mathcal{O}((N_c/N - 1)^0) \right). \quad (16)$$

The higher-order terms can be estimated from the numerical solution of the gap equation before linearization [10] as $\mathcal{O}((N_c/N - 1)^0) = C + \mathcal{O}(N_c/N - 1)$ with $C \approx 3.7$. The transition as a function of N displays an *essential singularity*, similar to the Kosterlitz-Thouless transition, and the mass gap is exponentially suppressed in the vicinity of the transition point. This justifies the linearization of the gap equation in order to calculate N_c .

V. DYNAMICAL SCREENING

Equations (10) and (11) imply that screening is not as efficient at higher frequencies $|\omega| \gg p^2$. As compared to the static approximation, one therefore expects the value of N_c to *increase* when dynamical screening effects are taken into account. We demonstrate next that this is indeed the case. The linearized gap equation that includes the full frequency dependence of the screened potential is given by

$$N\Delta(\omega, \vec{p}) = \int_{\nu, \vec{q}} \frac{\mathcal{F}\left(\sqrt{\frac{|\omega-\nu|}{(\vec{p}-\vec{q})^2}}\right)}{|\vec{p}-\vec{q}|(\nu^2 + q^4)} \Delta(\nu, \vec{q}), \quad (17)$$

and it defines a Fredholm eigenvalue equation in the space of integrable functions with appropriate boundary conditions. The corresponding integral kernel can be symmetrized by rescaling the gap function $\Delta(\omega, \vec{p})/\sqrt{\omega^2 + p^4} \mapsto \Delta(\omega, \vec{p})$:

$$N\Delta(\omega, \vec{p}) = \int_{\nu, \vec{q}} k(\omega, \vec{p}; \nu, \vec{q}) \Delta(\nu, \vec{q}), \quad (18)$$

with $k(\omega, \vec{p}; \nu, \vec{q}) = \mathcal{F}\left(\sqrt{\frac{|\omega-\nu|}{(\vec{p}-\vec{q})^2}}\right)/[|\vec{p}-\vec{q}|\sqrt{(\nu^2 + q^4)(\omega^2 + p^4)}]$, and the spectrum of the integral operator defined by k is thus real. Each of its eigenvectors represents a nontrivial solution to the gap equation, and the critical fermion number N_c is hence given by the operator's *largest eigenvalue* μ_{\max} .

A lower bound on the value of N_c can be found by recognizing that the *Rayleigh quotient*

$$R(k, \Delta) = \frac{\langle \Delta | k | \Delta \rangle}{\langle \Delta | \Delta \rangle} \equiv \frac{\int_{\omega, \vec{p}, \nu, \vec{q}} \Delta(\omega, \vec{p}) k(\omega, \vec{p}; \nu, \vec{q}) \Delta(\nu, \vec{q})}{\int_{\omega, \vec{p}} \Delta(\omega, \vec{p}) \Delta(\omega, \vec{p})}$$

is bounded from above by $R(k, \Delta) \leq \mu_{\max} = N_c$. This allows a variational approach in which $R(k, \Delta)$ is maximized within a suitable set of test functions. As proof of concept, we employ this method first for the static approximation, where the corresponding integral kernel is given by $k^{(0)}(p, q) = 4/[3\pi(\pi - 2)\max(p, q)]$. In this case, we can construct an optimal set of variational functions from the known solution (15). We choose $\Delta_\alpha^{(0)}(p) = \sin[\alpha \log(\frac{p}{\lambda})]/\sqrt{p}$, with variational parameter α and IR cutoff λ . For $\Lambda/\lambda \gg 1$ the Rayleigh quotient is maximized when $\alpha \rightarrow 0$, and it has the asymptotic form

$$R(k^{(0)}, \Delta_{\alpha \rightarrow 0}^{(0)}) \simeq \frac{16}{3\pi(\pi - 2)} \left(1 - \frac{3}{\ln(\frac{\Lambda}{\lambda})} + \frac{24}{\ln^3(\frac{\Lambda}{\lambda})}\right), \quad (19)$$

depicted in Fig. 1. In the limit $\Lambda/\lambda \rightarrow \infty$ the variational method approaches the correct static-approximation result $N_c = 16/[3\pi(\pi - 2)]$, consistent with the fact that our ansatz contains the solution (15).

In order to take the dynamical screening effects into account, we use the related ansatz $\Delta_\alpha(\omega, \vec{p}) =$

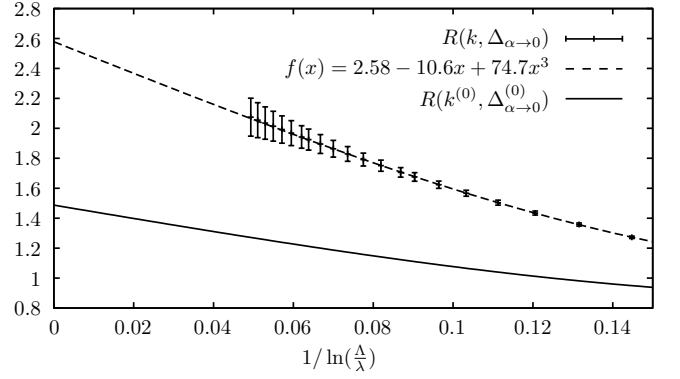


FIG. 1. Rayleigh quotient R for $\alpha \rightarrow 0$ as a function of the cutoff ratio Λ/λ in static approximation (solid line) and when dynamical screening effects are taken into account (data points). For the latter, the polynomial fit $f(x) = f_0 + f_1x + f_3x^3$ (dashed line) yields $N_c \geq f_0 = 2.6(2)$.

$\Delta_\alpha^{(0)}(|\vec{p}|)/\sqrt{\omega^2 + p^4}$, chosen such that the static solution would be recovered if dynamical screening were again neglected in the kernel. To obtain a lower bound on N_c , we may furthermore approximate the scaling function involved in $k(\omega, \vec{p}; \nu, \vec{q})$ by its lower bound $\mathcal{F}(x) \geq \mathcal{F}_0(x) = a\sqrt{1+x^2}$, with optimized coefficient $a \simeq 12.17$, allowing us to carry out the spherical integrals analytically. The result of the remaining numerical integrations over frequencies $|\omega|, |\nu| \in (\lambda^2, \Lambda^2)$ and momenta $p, q \in (\lambda, \Lambda)$ is displayed in Fig. 1 as a function of the cutoff ratio Λ/λ , for the optimized variational parameter $\alpha \rightarrow 0$. As expected, we find the Rayleigh quotient, and therefore N_c , to be significantly larger than in the static approximation. The data points are fitted well by a third-order polynomial inspired from Eq. (19), enabling us to extrapolate to $\Lambda/\lambda \rightarrow \infty$. This way we obtain a lower bound for the critical fermion number with the dynamical screening effects included: $N_c \geq 2.6(2)$, and thus significantly above $N = 1$ [31].

VI. EXPERIMENTAL IMPLICATIONS

The low-temperature ground state is consequently described by the mean-field Hamiltonian $\mathcal{H}_{\text{mf}} = \mathcal{H}_0 + \Delta_0 \gamma_5$, with $\Delta_0 \equiv \Delta(0, 0) > 0$. The spectrum of \mathcal{H}_{mf} is fully gapped, with the minimal gap in the p_x - p_y plane. In fact, \mathcal{H}_{mf} describes a QBT system that appears as if under “dynamically generated” uniaxial strain [2, 7, 32], with the rotational symmetry being *spontaneously* broken. Strained HgTe, however, is well-known as a strong topological insulator [2, 4]. Without external strain, clean HgTe and its analogs hence become at low temperatures strong topological *Mott* insulators [9, 33]. Equation (16) allows to estimate the Mott gap: $\Delta_0 \sim \varepsilon_* \exp(-4\pi/\sqrt{N_c/N - 1} + C) \gtrsim \varepsilon_*/500$ when $N_c \geq 2.6$, with ε_* the characteristic energy scale for interaction effects. For HgTe and α -Sn it is $\varepsilon_* \sim \mathcal{O}(1 \text{ meV})$ [1],

but larger for $\text{Pr}_2\text{Ir}_2\text{O}_7$ [6]. Experimentally, the transition manifests itself, for instance, in the temperature dependence of the Hall coefficient R_H , which turns from polynomial form $R_H \propto T^{-3/2}$ above $T_c \sim \varepsilon_*/500k_B$ to an exponential dependence $R_H \propto \exp(\Delta_0/k_B T)$ below T_c . Similar behavior is expected for the diagonal part of the electrical conductivity, which should also inherit the anisotropy of the spectrum when $T < T_c$.

In uniform magnetic fields \vec{h} energetics suggests that the dynamically induced “strain” aligns parallel to \vec{h} , and is described by

$$\mathcal{H}_{\text{mf+h}} = \mathcal{H}_0 + \Delta_0 \gamma_5 + h (J_z \cos \theta + J_z^3 \sin \theta), \quad (20)$$

Here, $J_z = i\gamma_3\gamma_4 + \frac{i}{2}\gamma_1\gamma_2$, and θ controls the relative strength of the symmetry-allowed cubic Zeeman term. $\mathcal{H}_{\text{mf+h}}$ leads to a rich phase diagram, previously investigated in the context of the QBT system under external strain [7]. For small θ and $h > h_c \simeq \Delta_0/\mu_B$ two Weyl nodes with linear dispersion along the p_z axis and quadratic dispersion perpendicular to it emerge in the spectrum—a pristine *double-Weyl* semimetal phase [34]. By increasing h even further, the Weyl points are shifted away from the Fermi level and the system becomes metallic with coexisting Fermi pockets. Across this transition the magnetic Grüneisen ratio [35] is conjectured to display a sign change [7]. When θ is larger, the transition for increasing h is towards a normal metal, before eventually the Weyl nodes again emerge. The gapless non-Fermi-liquid state, by contrast, turns into a Weyl (semi)metal already at infinitesimal magnetic field and should not allow any transition at finite h as long as θ cannot be tuned experimentally [7].

VII. CONCLUSIONS

We argued that the 3D gapless semiconductors with N points of quadratic band touching at the Fermi level exhibit a universal critical fermion number N_c below which the Abrikosov-Beneslavskii non-Fermi-liquid state becomes unstable. To leading order in the $1/N$ expansion we find $N_c = 16/[3\pi(\pi - 2)]$ in the static approximation, and even larger when dynamical screening effects are taken into account. From the experience gained in the related situation in QED_3 [11, 12], we expect that our main qualitative result $N_c > 1$ is robust upon inclusion of higher-order corrections in $1/N$. At low temperatures, clean HgTe and its analogs consequently should suffer a phase transition towards a state with spontaneously broken rotational symmetry, and with a full but anisotropic gap in the spectrum—a topological Mott insulator phase.

We have here limited ourselves to an isotropic model, which appears to be a valid low-energy description for HgTe and $\alpha\text{-Sn}$, and it leads to the nematic ordering as dominant instability. In the pyrochlore iridates that exhibit a magnetic transition, however, quantum fluctuations may induce significant anisotropies [22]. In that case, a mass gap that anticommutes with the effective (anisotropic) Hamiltonian is possible, in contrast to the isotropic case, and hence might be favored. It can be understood as an order parameter for the antiferromagnetic all-in/all-out instability [22], and we therefore believe that a similar scenario as developed in the present work might be relevant also for the transitions found experimentally in the pyrochlores [36].

ACKNOWLEDGMENTS

The authors thank B. Skinner for discussions and acknowledge support by the DFG under Grants No. JA2306/1-1 and No. JA2306/3-1, as well as the NSERC of Canada. Numerical integrations were performed in C using the CUBA library [37].

-
- [1] I. M. Tsvelik, *Electron Spectrum of Gapless Semiconductors* (Springer-Verlag, Berlin, 1997), Chap. 3.
 - [2] L. Fu and C. L. Kane, Phys. Rev. B **76**, 045302 (2007).
 - [3] M. König, S. Wiedmann, C. Brüne, A. Roth, H. Buhmann, L. W. Molenkamp, X.-L. Qi, and S.-C. Zhang, Science **318**, 766 (2007).
 - [4] C. Brüne, C. X. Liu, E. G. Novik, E. M. Hankiewicz, H. Buhmann, Y. L. Chen, X. L. Qi, Z. X. Shen, S.-C. Zhang, and L. W. Molenkamp, Phys. Rev. Lett. **106**, 126803 (2011).
 - [5] W. Witczak-Krempa, G. Chen, Y. B. Kim, and L. Balents, Ann. Rev. Cond. Matt. Phys. **5**, 57 (2014), and references therein.
 - [6] T. Kondo, M. Nakayama, R. Chen, J. J. Ishikawa, E.-G. Moon, T. Yamamoto, Y. Ota, W. Malaeb, H. Kanai, Y. Nakashima, Y. Ishida, R. Yoshida, H. Yamamoto, M. Matsunami, S. Kimura, N. Inami, K. Ono, H. Kumigashira, S. Nakatsuji, L. Balents, S. Shin, Nat. Commun. **6**, 10042 (2015).
 - [7] E.-G. Moon, C. Xu, Y. B. Kim, and L. Balents, Phys. Rev. Lett. **111**, 206401 (2013).
 - [8] A. A. Abrikosov and S. D. Beneslavskii, Sov. Phys. JETP **32**, 699 (1971); A. A. Abrikosov, *ibid.* **39**, 709 (1974).
 - [9] I. F. Herbut and L. Janssen, Phys. Rev. Lett. **113**, 106401 (2014).
 - [10] T. Appelquist, D. Nash, and L. C. R. Wijewardhana, Phys. Rev. Lett. **60**, 2575 (1988).
 - [11] D. Nash, Phys. Rev. Lett. **62**, 3024 (1989); T. Appelquist, J. Terning, and L. C. R. Wijewardhana, *ibid.* **75**, 2081 (1995).

- [12] P. Maris, Phys. Rev. D **54**, 4049 (1996); C. S. Fischer, R. Alkofer, T. Dahm, and P. Maris, *ibid.* **70**, 073007 (2004).
- [13] T. Grover, Phys. Rev. Lett. **112**, 151601 (2014).
- [14] J. Braun, H. Gies, L. Janssen, and D. Roscher, Phys. Rev. D **90**, 036002 (2014).
- [15] N. W. Ashcroft and N. D. Mermin, *Solid State Physics*, (Holt, Rinehart and Winston, Philadelphia, 1976), Chap. 17.
- [16] B. I. Halperin and T. M. Rice, Rev. Mod. Phys. **40**, 755 (1968).
- [17] L. D. Landau and E. M. Lifshitz, *Quantum Mechanics: Non-relativistic Theory* (Pergamon Press, Oxford, 1977), Sec. §35.
- [18] A. M. Essin and D. J. Griffiths, Am. J. Phys. **74**, 109 (2006); D. B. Kaplan, J.-W. Lee, D. T. Son, and M. A. Stephanov, Phys. Rev. D **80**, 125005 (2009), and references therein.
- [19] H. E. Camblong, L. N. Epele, H. Fanchiotti, and C. A. Garcia Canal, Phys. Rev. Lett. **87**, 220402 (2001).
- [20] J. M. Luttinger, Phys. Rev. **102**, 1030 (1956).
- [21] S. Murakami, N. Nagaosa, and S.-C. Zhang, Phys. Rev. B **69**, 235206 (2004).
- [22] L. Savary, E.-G. Moon, and L. Balents, Phys. Rev. X **4**, 041027 (2014).
- [23] L. Janssen and I. F. Herbut, Phys. Rev. B **92**, 045117 (2015).
- [24] I. F. Herbut, V. Juričić, B. Roy, Phys. Rev. B **79**, 085116 (2009); S. Ryu, C. Mudry, C.-Y. Hou, and C. Chamon, *ibid.* **80**, 205319 (2009); I. F. Herbut, *ibid.* **85**, 085304 (2012).
- [25] K. Sun, H. Yao, E. Fradkin, and S. A. Kivelson, Phys. Rev. Lett. **103**, 046811 (2009); B. Dóra, I. F. Herbut, and R. Moessner, Phys. Rev. B **90**, 045310 (2014).
- [26] D. V. Khveshchenko, Phys. Rev. Lett. **87**, 246802 (2001); D. V. Khveshchenko and H. Leal, Nucl. Phys. **B687**, 323 (2004); D. V. Khveshchenko, J. Phys. Condens. Matter **21**, 075303 (2009).
- [27] E. V. Gorbar, V. P. Gusynin, V. A. Miransky, and I. A. Shovkovy, Phys. Rev. B **66**, 045108 (2002); O. V. Gamayun, E. V. Gorbar, and V. P. Gusynin, *ibid.* **81**, 075429 (2010).
- [28] C. Popovici, C. S. Fischer, and L. von Smekal, Phys. Rev. B **88**, 205429 (2013).
- [29] The effects of the band mass renormalization are expected to only affect the energy scale at which a possible excitonic transition takes place, but not the value of N_c itself, cf. Ref. [28].
- [30] R. Fukuda and T. Kugo, Nucl. Phys. **B117**, 250 (1976).
- [31] Note that the displayed uncertainty for N_c includes only the error from numerical integration and extrapolation, but not the systematic error from neglecting the unknown corrections of higher order in $1/N$.
- [32] B. J. Roman and A. W. Ewald, Phys. Rev. B **5**, 3914 (1972).
- [33] S. Raghu, X.-L. Qi, C. Honerkamp, and S.-C. Zhang, Phys. Rev. Lett. **100**, 156401 (2008).
- [34] G. Xu, H. Weng, Z. Wang, X. Dai, and Z. Fang, Phys. Rev. Lett. **107**, 186806 (2011); C. Fang, M. J. Gilbert, X. Dai, and B. A. Bernevig, Phys. Rev. Lett. **108**, 266802 (2012); S.-M. Huang, S.-Y. Xu, I. Belopolski, C.-C. Lee, G. Chang, B. Wang, N. Alidoust, M. Neupane, H. Zheng, D. Sanchez, A. Bansil, G. Bian, H. Lin, M. Z. Hasan, Proc. Natl. Acad. Sci. U.S.A. **113**, 1180 (2016).
- [35] L. Zhu, M. Garst, A. Rosch, and Q. Si, Phys. Rev. Lett. **91**, 066404 (2003).
- [36] H. Sagayama, D. Uematsu, T. Arima, K. Sugimoto, J. J. Ishikawa, E. O'Farrell, and S. Nakatsuji, Phys. Rev. B **87**, 100403 (2013); K. Tomiyasu, K. Matsuhira, K. Iwasa, M. Watahiki, S. Takagi, M. Wakeshima, Y. Hinatsu, M. Yokoyama, K. Ohoyama, and K. Yamada, J. Phys. Soc. Jpn. **81**, 034709 (2012).
- [37] T. Hahn, Comput. Phys. Commun. **168**, 78 (2005).